PCCP
Physical Chemistry Chemical Physics

# Accepted Manuscript

This article can be cited before page numbers have been issued, to do this please use: I. Lelidis and G. Barbero, *Phys. Chem. Chem. Phys.*, 2026, DOI: 10.1039/D6CP01514J.




ROYAL SOCIETY OF CHEMISTRY

rsc.li/pccp

View Article Online
DOI: 10.1039/D6CP01514J

# Effect of adsorption on the electrostatic behavior of an electrolytic cell

Ioannis Lelidis[1,*] and Giovanni Barbero[2,3]

[1] *Department of Condensed Matter Physics, Faculty of Physics, National and Kapodistrian University of Athens, Panepistimiopolis, 15784 Zografos, Athens, Greece*

[2] *Department of Applied Science and Technology, Politecnico di Torino, Corso Duca degli Abruzzi 24, 10129 Torino, Italy*

[3] *Istituto dei Sistemi Complessi (ISC–CNR), Via dei Taurini 19, 00185 Rome, Italy*





*corresponding author's email: ilelidis@phys.uoa.gr

View Article Online
DOI: 10.1039/D6CP01514J






## Abstract

Understanding the interplay between bulk electrostatics and surface adsorption is crucial for optimizing the performance of electrochemical devices, sensors, and soft materials such as hydrogels. The present study aims to determine how ionic adsorption, both in the absence and presence of an external bias voltage, affects equilibrium ion distributions and electrostatic properties, within the framework of the Poisson-Nernst-Planck model. The analysis is performed assuming that the kinetic equation, describing the adsorption-desorption phenomenon, is well approximated by a Langmuir isotherm, containing an adsorption term proportional to the bulk density of adsorbate particles just in front of the adsorbent surface, and a desorption term proportional to the adsorbed particles. The system is modeled as a slab with only ions of a given sign mobile. We consider both symmetric and asymmetric electrolytic cells under open-circuit, short-circuit and externally applied bias conditions. We determine the equilibrium bulk ion distributions, electric field and potential profiles, as well as the surface density of adsorbed ions and the surface fields and potentials. The limit of non interacting surfaces was investigated. The results provide insight into the coupling between surface processes and bulk electrostatics in complex ionic systems.


## I. INTRODUCTION

Liquids usually contain ions, originating either from the fabrication process or from the spontaneous thermal dissociation of neutral particles. In an infinite system, at thermodynamic equilibrium, the liquid is globally and locally electrically neutral. When the liquid is confined by surfaces, adsorption mechanisms related to surfaces forces may push the ions toward or away from the interfaces [1–3]. In this case, the liquid remains globally electrically neutral but can become locally charged if the adsorption for positive and negative ions differs. Adsorption is widely studied and exploited in liquid crystals [4–6], colloids [7–9], polymers [10–12], electrocatalysis [13], electrochemistry [14, 15], proteins [16–18], environmental [19, 20], energy storage [21, 22], and industrial technologies due to its ability to selectively remove, separate, or concentrate species at interfaces [23, 24]. The surface charge at the electrodes created by adsorption, even in the absence of Faradaic reactions, alters the equilibrium potential profile and if the electrolytic cell is asymmetric (non-identical electrodes) then a finite equilibrium potential difference appears at open-circuit conditions [25].

View Article Online
DOI: 10.1039/D6CP01514J





The induced electric potential difference, due to the adsorption phenomenon, has significant technological implications [26]. Moreover, adsorption-desorption kinetics couples to the bulk ion transport giving rise to additional relaxation modes. These effects have been revealed mainly by impedance spectroscopy [27–30] and capacitance measurements at low frequencies [4].

The aim of this paper is to investigate the potential difference between the electrodes of an electrolytic cell and to analyze the role of an external bias applied by means of a power supply, on the bulk ionic density distribution, internal electric field, and electric potential across the cell. The present paper represents a natural extension of the work by Bousiadi and Lelidis [25]. Here the analysis is performed for symmetric and asymmetric electrolytic cells under open circuit, external bias, and short circuit conditions. The analysis is performed using the Poisson-Nernst-Planck (PNP) model [31–33], based on the continuity equations for positive and negative ions and on Poisson equation, which relates the actual electric potential to the ionic charge distribution. For the sake of simplicity, we restrict our analysis to a system in which only the positive ions are mobile, as in hydrogels [34, 35], and assume that the adsorption phenomenon is well described by Langmuir kinetics [4, 36–38]. Moreover, the sample is supposed to have the shape of a slab to reduce the mathematical problem to one dimension. We further limit our investigation to the static case where the system, composed by the liquid plus the adsorbent surfaces, has reached equilibrium, after a transient time. In this limit, the surface density of adsorbed ions is proportional to the bulk density of the adsorbate particles, just in front of the adsorbent surface. The density of ions is supposed small in respect to the density of the liquid molecules and therefore association-dissociation effects can be neglected [39]. Since only cations are mobile the ambipolar diffusion mechanism is not activated [41].

Our analysis is performed within the continuum approximation, in which bulk and surface charges are described by bulk and surface densities of charge. The basic assumptions are: (1) the ions are treated as point charges; (2) the bulk and surface charges are assumed to be uniformly smeared in the bulk and over the surfaces; and (3) the electrolyte solution is described as a continuum with a uniform dielectric constant. From these hypotheses, it follows that the distance between the ions in the bulk and at the surface are very small compared to the characteristic length scales of the problem, that is, the sample thickness, the Debye length, and the dimensions of the limiting surfaces [31]. In this approximation, the ions

View Article Online
DOI: 10.1039/D6CP01514J





are represented by fields of bulk densities: uniform for the negative charges, and position dependent for the positive ones. The electric field created by the ions is described by the spatial average of the actual microscopic field, as usual in macroscopic electrodynamics [40]. The finite size of the ions is taken into account through the phenomenological parameters describing their diffusion and electric mobility in the medium where they are dispersed, by means of the Stokes relations [36]. However, our description remains at the continuum level, and these aspects of the problem are not addressed. The same considerations apply to the description of the adsorption phenomenon. Adsorption is related to the interaction energy of a particle with the substrate. It originates from the direct interaction of the ion with its electric image in the substrate and from van der Waals interactions [40]. These interactions depend on the molecular properties of the ions, the molecular properties of the medium in which they are dispersed and of the substrate, through the frequency dispersion of the dielectric constant [40], on the density of adsorption sites and the geometrical dimensions of the ions. In our model, the adsorption is described only by two phenomenological parameters, along the line suggested by Langmuir [1]. In the limit of weak adsorption, saturation effects can be neglected, and Langmuirâs model is expected to provide a good approximation.

Within this framework, the effects of the external field on the equilibrium distributions of ion densities in the bulk and at the surface, as well as on the macroscopic electric field, are investigated. In particular, it is discussed the half-space approximation (HSA) regime, corresponding to the case in which the thickness of the sample is very large with respect to the Debye length. The opposite limit, where the thickness of the cell is much smaller than the Debye length, corresponding to a liquid that can be considered as a perfect insulator, is also discussed in the continuum approximation used in our analysis.

The proposed analysis is applicable to a variety of systems where surface interactions influence electrostatics. These include electrochemical devices such as batteries, supercapacitors, metal-organic frameworks, and electrosorption cells, where surface adsorption determines charge storage and potential profiles; polyelectrolyte films, ion-conducting membranes, and hydrogels, where mobile counterions interact with functionalized surfaces; charged colloids and functionalized nanoparticles, where adsorption modifies zeta potential and interparticle forces; and biointerfaces, lipid membranes, and microfluidic channels, where adsorption-induced surface potentials impacts transport, sensing, and electrokinetic behavior [42–48].

This work is motivated for two main reasons: i) to account for real electrodes where

View Article Online
DOI: 10.1039/D6CP01514J





adsorption and desorption occur, which is relevant for electrochemical systems, soft-matter, colloidal dispersions, bio-interfaces, hydrogels and polyelectrolytes, which rarely have perfectly blocking or inert interfaces, and ii) to propose a unified theoretical framework to treat the electrostatic behavior of an open-circuit, short-circuit, grounded, biased or unbiased, symmetric or asymmetric electrolytic cells, which is lacking in the literature.

## II. FUNDAMENTAL EQUATIONS OF THE PROBLEM

The quantities characterizing the system are the bulk density of mobile ions $n$, the surface density of adsorbed ions, $s$, the electric field $F$, and the relevant electric potential $U$. In the absence of adsorption the liquid is assumed globally and locally neutral, with a bulk density of mobile ions $n_0$ position independent, identical to that of negative ions, fixed in space. The sample is supposed in the shape of a slab of thickness $d$. The cartesian reference frame used for the mathematical description has the $Z$-axis perpendicular to the limiting surfaces, at $Z = \pm d/2$. The quantities characterizing the system depend on the coordinate $Z$ and time $T$. The Debye length is $\Lambda = \sqrt{\varepsilon v_{\rm th}/(n_0 q)}$, where $\varepsilon$ is the dielectric constant of the liquid free of ions [49], $q$ the electric charge of the mobile ions, and $v_{\rm th} = k_B\Theta/q$, where $\Theta$ is the absolute temperature, is the thermal voltage (of the order of 25 mV for monovalent ions). Debye's relaxation time $\tau_0$ is defined by $\tau_0 = \Lambda^2/D$, where $D$ is the diffusion coefficient of the mobile ions in the considered liquid.

The kinetic equations describing the adsorption phenomenon are assumed to be

$$\frac{ds_{p,m}}{dT} = \kappa_{p,m}\, n_{p,m}(T) - \frac{1}{\tau_{p,m}}\, s_{p,m}(T), \tag{1}$$

where $s_{p,m} = s(\pm d/2)$, $n_{p,m}(T) = n(\pm d/2, T)$, and $\kappa_{p,m}$ and $\tau_{p,m}$ are the adsorption coefficients and desorption times of the surfaces at $Z = \pm d/2$, respectively [42, 50–54]. From (1) it follows that the quantities

$$\ell_{p,m} = \kappa_{p,m}\, \tau_{p,m}, \tag{2}$$

have the dimension of a length, and are related to the penetration lengths of the surface forces responsible for the adsorption phenomenon.

Since the problem involves an intrinsic length, $\Lambda$, and an intrinsic time, $\tau_0$, we henceforth describe the system using dimensionless spatial and temporal variables defined as $z = Z/\Lambda$

View Article Online
DOI: 10.1039/D6CP01514J





and $t = T/\tau_0$. In terms of the reduced coordinate, the bounding surfaces are located at $z = \pm M$, where $M = d/(2\Lambda)$.

The system is characterized by the dimensionless quantities $N = n/n_0$, $S = s/(n_0\Lambda)$, and $E = \Lambda F/v_{\rm th}$. As it is evident from the definition, $N$ is the bulk density of particles measured in terms of $n_0$, the bulk density of particles in thermodynamical equilibrium, $S$ is the surface density of adsorbed particles measured in $n_0\Lambda$, the surface density of adsorbed particles in the Debye surface layer, $E$ is the electric field measured in terms of $v_{\rm th}/\Lambda$, and $V = U/v_{\rm th}$.

As discussed in [25], the fundamental equations of the problem are the equation of continuity for the mobile ions and the equation of Poisson for the electric potential across the cell

$$\frac{\partial N}{\partial t} = \frac{\partial^2 N}{\partial z^2} - \frac{\partial E}{\partial z}, \tag{3}$$

$$\frac{\partial E}{\partial z} = N - 1, \tag{4}$$

to be solved with the boundary conditions (BCs), at $z = \pm M$,

$$J(\pm M, t) = -\left(\frac{\partial N}{\partial z} - E\right)_{z=\pm M} = \pm \frac{dS_{p,m}}{dt}. \tag{5}$$

where $S_p$ and $S_m$ indicate the dimensionless surface densities on the surfaces at $z = \pm M$, and $J$ is the current density of mobile particles, due to the diffusion and drift, in dimensionless form. Finally, the kinetic equation (1) can be rewritten, in reduced units, as

$$\frac{dS_{p,m}}{dt} = a_{p,m} N(\pm M, t) - \frac{1}{b_{p,m}} S_{p,m}(t), \tag{6}$$

where $a_{p,m} = \kappa_{p,m}\tau_0/\Lambda$, and $b_{p,m} = \tau_{p,m}/\tau_0$. From the definition of $a_{p,m}$ it is evident that in the problem under consideration there is an intrinsic adsorption coefficient $\Lambda/\tau_0$.

In our analysis we are interested in the static behavior of the cell, where the quantities characterizing the system are time independent. For $\partial N/\partial t = 0$, and substituting equation (4) in (3) we get

$$\frac{d^2 N}{dz^2} - (N - 1) = 0, \tag{7}$$

with the BCs: $J(\pm M) = 0$, which simply state the conservation of the number of mobile ions, and it is equivalent to

$$S_m + S_p + \int_{-M}^{M} N(z)\, dz = 2M. \tag{8}$$

View Article Online
DOI: 10.1039/D6CP01514J





Finally, at static regime, from the kinetic equations (6), it follows that

$$S_j = \xi_j N_j, \tag{9}$$

where $j = p, m$, $N_{p,m} = N(\pm M)$, and $\xi_j = a_j\, b_j = \ell_j/\Lambda$. Equations (9) indicate that, in the considered approximation, the surface densities of adsorbed particles in the equilibrium state are proportional to the bulk densities of adsorbate particles just in front of the adsorbent surface. The proportionality factor $\xi_j$, is a length normalized by the Debye length and it will henceforth be called the adsorption length (in reduced, $\xi_j$, or absolute units, $\ell_j$). Apparently, the adsorption length is related to both the surface and volume properties of the system.

## III. SOLUTION IN THE STATIC REGIME

The solution of (7) is given by

$$N(z) = 1 + A\, \sinh[z] + B\, \cosh[z], \tag{10}$$

where $A$ and $B$ are two integration constants to be determined by means of the boundary conditions $J(\pm M) = 0$. From (4), taking into account (10) we get for the electric field

$$E(z) = A\, \cosh[z] + B\, \sinh[z] + C_0, \tag{11}$$

where $C_0$ is a new integration constant. Finally, the electric potential defined by $E = -dV/dz$, is found to be

$$V(z) = -A\, \sinh[z] - B\, \cosh[z] - C_0\, z + C_1, \tag{12}$$

with $C_1$ a new integration constant.

From (10), the surface values of the bulk densities of mobile ions are

$$N_{p,m} \;=\; 1 \pm A\, \sinh[M] + B\, \cosh[M], \tag{13}$$

the surface values of the electric field are

$$E_{p,m} \;=\; A\, \cosh[M] \pm B\, \sinh[M] + C_0, \tag{14}$$

and the surface values of the electric potential are

$$V_{p,m} \;=\; \mp A\, \sinh[M] - B\, \cosh[M] \mp C_0\, M + C_1. \tag{15}$$

View Article Online
DOI: 10.1039/D6CP01514J





In the absence of an external power supply the surface values of the electric field are related, for Gauss theorem, to the surface densities of adsorbed ions

$$E_m = S_m, \quad \text{and} \quad E_p = -S_p, \tag{16}$$

where the surface densities of adsorbed particles are given by (9).

The condition on the conservation of mobile particles (8) can now be rewritten as

$$K = S_m + S_p + 2\,B\,\sinh[M] = 0 \tag{17}$$

The integration constants $A$, $B$, $C_0$ and $C_1$ are determined imposing the boundary conditions (16,17) and that the current density across the sample vanishes identically. In particular, the integration constant $C_1$ depends on the potential reference, and in the absence of the external power supply can be put $C_1 = 0$.

## IV. ASYMMETRIC SLAB

For open circuit conditions, we consider first the case in which the slab is limited by two different adsorbing surfaces, i.e., $a_m \neq a_p$, $b_m \neq b_p$, and $a_m b_m \neq a_p b_p$. In this case, the integration constants are: $C_0 = 0$,

$$A = -\frac{\Delta\xi}{\Pi}\,\sinh[M], \quad \& \quad B = -\frac{(\xi_m + \xi_p)\cosh[M] + 2\xi_m\xi_p \sinh[M]}{\Pi}, \tag{18}$$

where $\Pi = (\xi_m + \xi_p)\cosh[2M] + (1 + \xi_p\xi_m)\sinh[2M]$, and $\Delta\xi = \xi_p - \xi_m$.

Substituting the above expressions into (10,11,12), the expressions for $N(z)$, $E(z)$ and $V(z)$ are obtained as follows

$$N(z) = 1 - \frac{\Delta\xi \sinh[M]\sinh[z] + [(\xi_m + \xi_p)\cosh[M] + 2\xi_m\xi_p \sinh[M]]\cosh[z]}{\Pi} \tag{19}$$

$$E(z) = -\frac{\Delta\xi \sinh[M]\cosh[z] + [(\xi_p + \xi_m)\cosh[M] + 2\xi_p\xi_m \sinh[M]]\sinh[z]}{\Pi} \tag{20}$$

$$V(z) = \frac{\Delta\xi \sinh[M]\sinh[z] + [(\xi_p + \xi_m)\cosh[M] + 2\xi_p\xi_m \sinh[M]]\cosh[z]}{\Pi} \tag{21}$$

These expressions show that, within the framework of the present model, the adsorption properties of the electrodes do not depend on the specific values of $a_j$ and $b_j$ but only from their product $a_j b_j$, that is, at the static regime, the electrodes can be treated as identical

View Article Online
DOI: 10.1039/D6CP01514J





provided they are characterized by the same adsorption length ($\xi_p = \xi_m$). The profiles of $N(z)$, $E(z)$ and $V(z)$, numerically calculated using the values $\xi_m = 6$, $\xi_p = 54$ and $M = 5$, are shown in Figures 1-3, respectively. Figures 1 and 2 show that the ion concentration and electric field profiles, respectively, are asymmetric with respect to the midplane of the cell. From Figure 3, it can be deduced that a non-zero electric potential difference, $\Delta V \neq 0$, exists between the electrodes under open-circuit conditions. These asymmetries arise from the different adsorption lengths at the cell electrodes.

The surface values of the bulk densities of mobile ions, $N_j$ are

$$N_{m,p} \;=\; 2(\cosh[M] + \xi_{p,m}\sinh[M])\,\frac{\sinh[M]}{\Pi}\,. \tag{22}$$

In the limit $M \to \infty$, i.e., when $d \gg \Lambda$, which corresponds to the HSA (denoted henceforth with the subscript "$l$"), from (22), we obtain

$$N_{jl} = \frac{1}{1+\xi_j}. \tag{23}$$

The surface values of the electric field, $E_j$, and its value in the midplane of the cell,

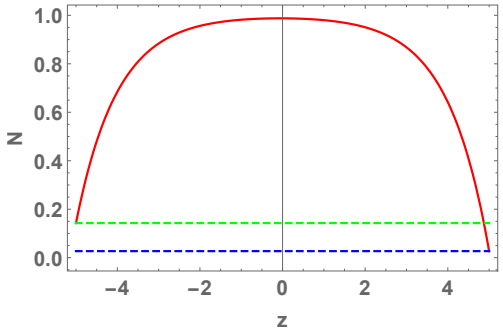


FIG. 1. Bulk density of mobile ions across the cell, in red, for $-M \le z \le M$. $\xi_m = 6$, $\xi_p = 54$ and $M = 5$. In green $N(-M) = N_m$, and in blue $N(M) = N_p$.

$E(z = 0) = E(0)$, are given by

$$E_{p,m} \;=\; \mp 2\,\frac{\xi_{p,m}\cosh[M] + \xi_p\xi_m\sinh[M]}{\Pi}\,\sinh[M], \tag{24}$$

$$E(0) \;=\; -\frac{\Delta\xi}{\Pi}\,\sinh[M]. \tag{25}$$

In the limit $M \to \infty$, (24,25) reduce to

$$E_{pl,ml} \;=\; \mp\frac{\xi_{p,m} + \xi_m\xi_p}{(\xi_m + \xi_p) + (1 + \xi_m\xi_p)}, \quad \text{and} \quad E_l(0) = 0. \tag{26}$$

View Article Online
DOI: 10.1039/D6CP01514J

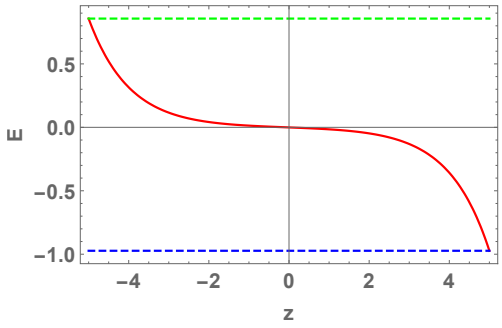


FIG. 2. Electric field across the cell due to the ionic adsorption, red curve, for $-M \leq z \leq M$. $\xi_m = 6$, $\xi_p = 54$ and $M = 5$. In green $E(-M) = E_m$, and in blue $E(M) = E_p$.

The surface values of the electric potential, $V_j$, and its value in the middle of the cell, V(0), are

$$V_{p,m} = \frac{\xi_{m,p} + \xi_{p,m}\cosh[2M] + \xi_p\xi_m \sinh[2M]}{\Pi}, \tag{27}$$

$$V(0) = \frac{(\xi_m + \xi_p)\cosh[M] + 2\xi_m\xi_p \sinh[M]}{\Pi}. \tag{28}$$

In the limit of $M \to \infty$, from (27,28) follow

$$V_{jl} = \frac{\xi_j}{1+\xi_j}, \quad \text{and} \quad V_l(0) = 0. \tag{29}$$

The potential difference, $\Delta V = V_p - V_m$, between the two electrodes due to the adsorption phenomenon, is given by

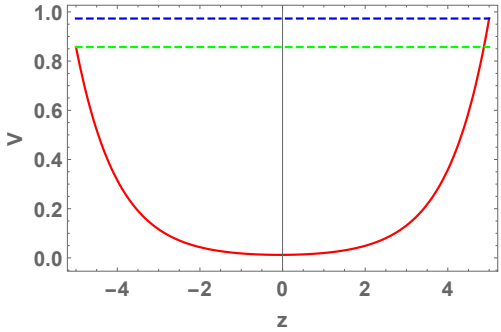


FIG. 3. Electric potential due to the ionic adsorption of ions across the cell, in red, for $-M \leq z \leq M$. In green $V(-M) = V_m$, and in blue $V(M) = V_p$. $\xi_m = 6$, $\xi_p = 54$ and $M = 5$.

$$\Delta V = -\frac{2\Delta\xi \sinh[M]^2}{\Pi} \tag{30}$$

View Article Online
DOI: 10.1039/D6CP01514J



which in the HSA reduces to

$$\Delta V_l = -\frac{\Delta\xi}{(1+\xi_p)(1+\xi_m)}, \tag{31}$$

as it follows also from (29).

Figure 4 depicts $\Delta V(M)$ calculated for $\xi_m = 12$ and $\xi_p = 6$. $\Delta V(M)$ reaches its maximum in the HSA ($d >> \Lambda$) and approaches zero in the limit $\Lambda >> d$, corresponding to a perfect insulator. A discussion of the physical meaning of Fig. 4, in particular in the limit of small $M$, is in order. We assume that the medium under consideration can be described by a continuum particle density. This implies that, in the bulk, the average distance between the ions, $R$, must be much smaller than both the sample thickness $d$ and the Debye length $\Lambda$. In equilibrium, the bulk ion density is $n_0$. Assuming the ions to be arranged on a cubic lattice of spacing $R$, we obtain $R = n_0^{-1/3}$. The condition $R \ll d$ then yields $n_0 \gg d^{-3}$, whereas the condition $R \ll \Lambda$ gives $n_0 \ll (4\pi\ell_B)^{-3}$, where $\ell_B = q/(4\pi\varepsilon\, v_{th})$ is the Bjerrum length, defined as the distance between two ions where the electrostatics interaction energy, $U_E = (1/4\pi\varepsilon)q^2/\ell_B$ equals the thermal energy, $U_T = k_BT$ [36]. It follows that, within the continuum description, the bulk ion density must satisfy $1/d^3 \ll n_0 \ll 1/(4\pi\ell_B)^3$, and hence $d \gg 4\pi\ell_B$. In term of $\ell_B$ the quantity $\Lambda$ can be written as $\Lambda = \sqrt{1/(4\pi n_0 \ell_B)}$. Consequently, in the continuum approximation, the parameter $M$ has to satisfy

$$\sqrt{\pi\frac{\ell_B}{d}} \ll M \ll \frac{d}{4\pi\ell_B},$$

and the limit $M \to 0$ lies outside the range of validity of our approximation. This limiting case should therefore be regarded only as a formal mathematical limit of the model.

In the HSA, the dependence of $\Delta V$ on the reduced adsorption length $\xi_p$ while keeping $\xi_m$ constant, is shown in Figure 5.

The surface densities of particles adsorbed on the limiting surfaces are $S_j = \xi_j N_j$. In the limit $M \to \infty$, $S_j$ reduce to $S_{jl} = \xi_j/(1+\xi_j)$.

## V. SYMMETRIC SLAB

In the case of a slab bounded by two identical adsorbing surfaces, $\xi_j = \xi$, the corresponding equations describing the sample can be easily deduced by those presented in the previous

View Article Online
DOI: 10.1039/D6CP01514J

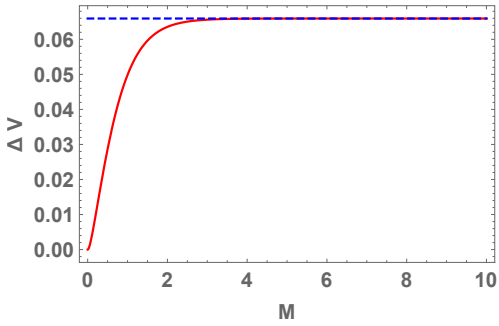


FIG. 4. Electric potential difference, $\Delta V$, between the adsorbing surfaces of the cell, versus $M = d/(2\Lambda)$. For $d \sim 5\Lambda$ the HSA works properly. $\xi_m = 12$, $\xi_p = 6$.

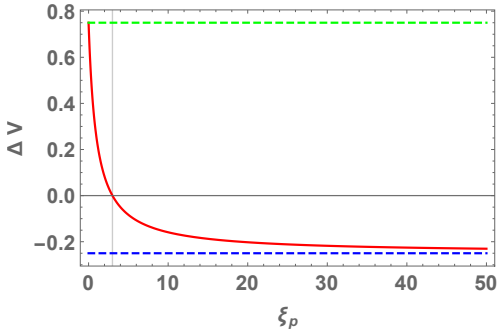


FIG. 5. Difference of electric potential, $\Delta V$ between the adsorbing surfaces of the cell versus $\xi_p$, for $\xi_m = 3$. The curve is drawn in the HSA, where $M \to \infty$. Note that for $\xi_m = \xi_p$, $\Delta V = 0$, as expected. The green dashed horizontal line represents $\Delta V$ in the HSA for $\xi_p = 0$, that is, when the surface at $z = M$ does not adsorb, and the blue one when $\xi_p \to \infty$ relevant to the case in which the adsorption at $z = M$ is very large with respect to that at $z = -M$.

section. In this case, the integration constants are

$$A = 0, \quad \& \quad B = -\frac{\xi}{\xi \cosh[M] + \sinh[M]}, \tag{32}$$

and the profiles of $N, E, V$ are given by

$$N(z) = 1 - \frac{\xi \cosh[z]}{\xi \cosh[M] + \sinh[M]}, \tag{33}$$

$$E(z) = -\frac{\xi \sinh[z]}{\xi \cosh[M] + \sinh[M]}, \tag{34}$$

$$V(z) = \frac{\xi \cosh[z]}{\xi \cosh[M] + \sinh[M]}. \tag{35}$$

The functions $N(z)$, $E(z)$ and $V(z)$ are shown in Figure 6 as blue dashed curves. For comparison, the corresponding red curves for an asymmetric cell are also plotted in the same

View Article Online
DOI: 10.1039/D6CP01514J



figure. Note that the blue curves, for a symmetric slab, exhibit a well defined symmetry in respect with the midplane of the cell, which is absent for the red curves of the asymmetric slab. Note also that the curves for both the symmetric and asymmetric cells appear to coincide in the right half of the cell, where the electrode for both cells has the same adsorption length. However, this is not the case, as can be inferred by comparing the corresponding equations. Simply, the influence of the asymmetry is strongly attenuated.

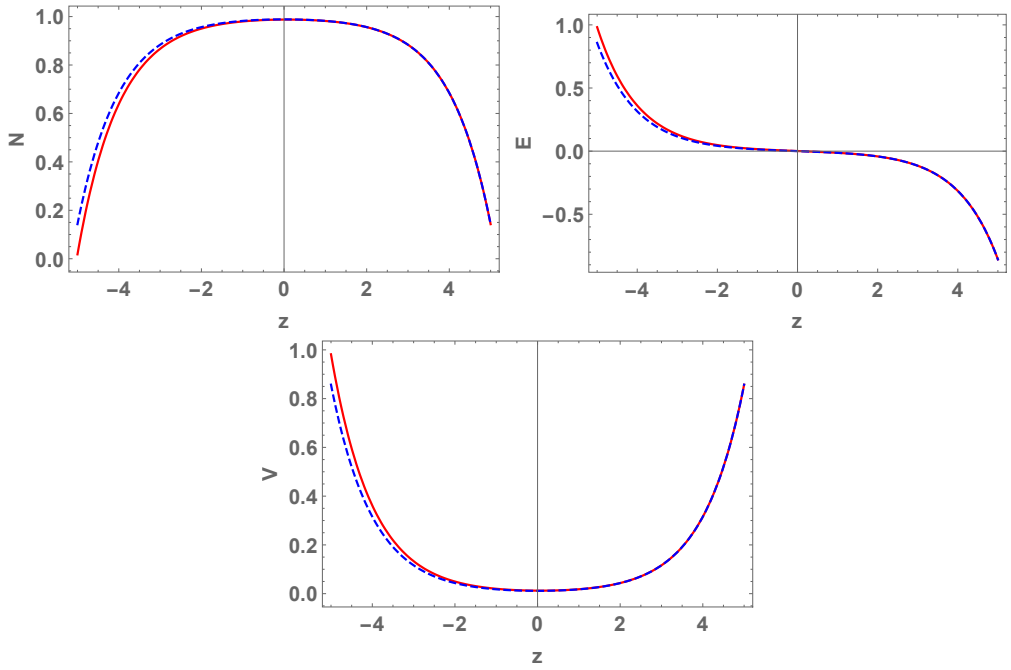


FIG. 6. Bulk ionic density of mobile ions $N$, electric field $E$, and electric potential $V$ across the cell thickness $z$, resulting from the adsorption of ions. $M = 5$. Blue dashed curves, symmetric cell with $\xi = 6$. Red curves, asymmetric cell with $\xi_p = 6$, $\xi_m = 54$.

From (33,34,35), the surface values of the bulk density of mobile ions, the electric field and the electric potential are given by

$$N_j = \frac{1}{1 + \xi \coth[M]}, \tag{36}$$

$$E_{m,p} = \pm \frac{\xi}{1 + \xi \coth[M]}, \tag{37}$$

$$V_j = \frac{\xi \cosh[M]}{\xi \cosh[M] + \sinh[M]}. \tag{38}$$

The surface densities of adsorbed ions are given by $S_j = \xi N_j$. The dependencies of the surface values of $N$, $E$, $V$ and of $S$ versus $M$ are shown in Figure 7. Note that the HSA

View Article Online
DOI: 10.1039/D6CP01514J

works well already for $M = 5$. In the HSA regime, (36,37,38) reduce to

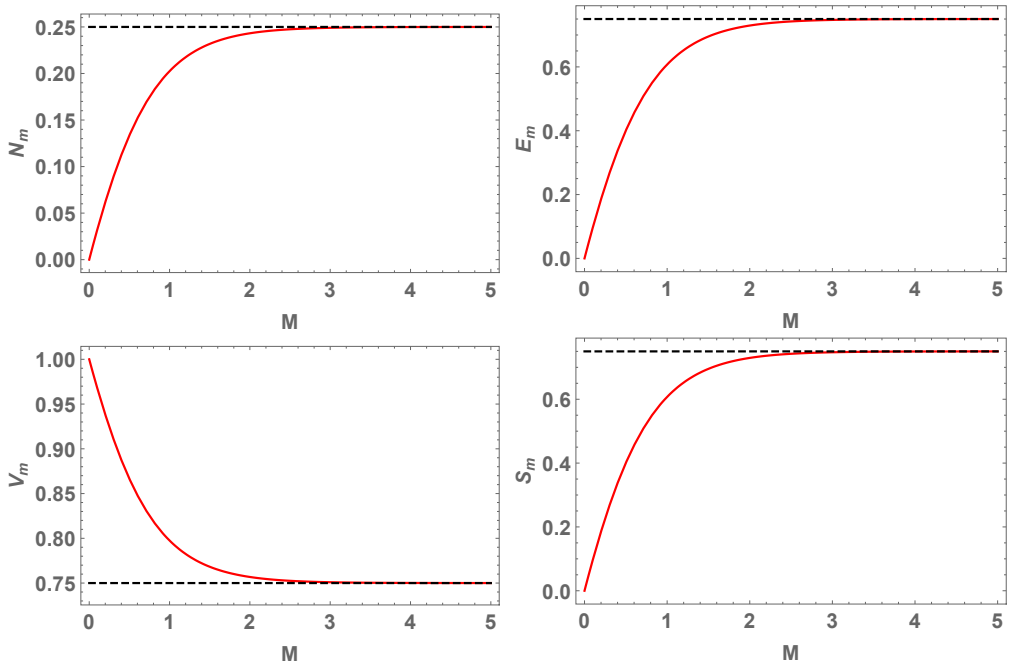


FIG. 7. Surface values of bulk density of mobile ions, $N_m$, electric field, $E_m$, electric potential, $V_m$, and surface density of adsorbed ions, $S_m$, vs. $M$, on the m-surface at $z = -M$ for a symmetric system. The curves are drawn for $\xi = 3$. The dashed lines, calculated from (39), correspond to the HSA.

$$S_j = V_j = \xi N_j = \frac{\xi}{1+\xi}, \quad E_{m,p} = \pm\frac{\xi}{1+\xi}. \tag{39}$$

## VI. SHORT-CIRCUITED ELECTRODES

When the electrodes are short-circuited (sc), they acquire the same potential $V_p = V_m$, and the integration constants then become: $C_0 = C_1 = A = 0$, and

$$B = -\frac{1}{\cosh[M] + 2\sinh[M]/(\xi_m + \xi_p)}. \tag{40}$$

View Article Online
DOI: 10.1039/D6CP01514J





The profiles of the bulk concentration ($N_{sc}$), electric field ($E_{sc}$), and potential ($V_{sc}$) reduce to:

$$N_{sc}(z) = 1 - \frac{(\xi_m + \xi_p)\cosh[z]}{(\xi_m + \xi_p)\cosh[M] + 2\sinh[M]}, \tag{41}$$

$$E_{sc}(z) = -\frac{(\xi_m + \xi_p)\sinh[z]}{(\xi_m + \xi_p)\cosh[M] + 2\sinh[M]}, \tag{42}$$

$$V_{sc}(z) = \frac{(\xi_m + \xi_p)\cosh[z]}{(\xi_m + \xi_p)\cosh[M] + 2\sinh[M]}. \tag{43}$$

Figure 8 shows $N_{sc}$, $E_{sc}$, $V_{sc}$ across the thickness of the cell. The corresponding surface

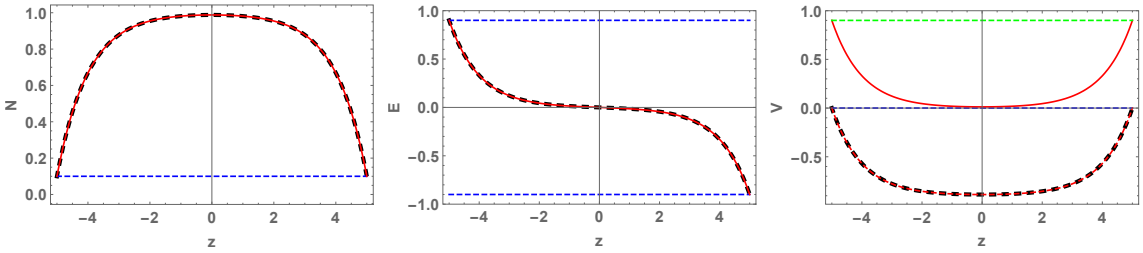


FIG. 8. $N_{sc}$, $E_{sc}$, $V_{sc}$ across a cell with short-circuited electrodes, red curves. The curves are drawn for $\xi_m = 3$ and $\xi_p = 15$ at $M = 5$. The blue and green horizontal dashed lines indicate the HSA regime values of the corresponding quantities. Black points concern grounded electrodes, that is, $V_0 = 0$. The red dashed curve is $V_{sc}$ shifted by the potential at the electrodes.

values, $N_{scj}$, $E_{scj}$, $V_{scj}$, are given by

$$N_{scj} = \frac{2}{2 + (\xi_m + \xi_p)\coth[M]}, \tag{44}$$

$$E_{scm} = -E_{scp} = \frac{\xi_m + \xi_p}{2 + (\xi_m + \xi_p)\coth[M]} \tag{45}$$

$$V_{scj} = \frac{(\xi_m + \xi_p)\cosh[M]}{(\xi_m + \xi_p)\cosh[M] + 2\sinh[M]}, \tag{46}$$

and they are shown in Figure 8 as dashed lines. Note that all the above results are independent of the symmetry of the cell with respect to the adsorption properties.

## VII. IN THE PRESENCE OF AN EXTERNAL FIELD

Let us consider now the case in which the sample is connected to an external power supply, fixing the potential of the adsorbing surfaces, playing the role of electrodes, at

$$V(\mp M) = V_{m,p} = \mp \frac{V_0}{2}. \tag{47}$$

View Article Online
DOI: 10.1039/D6CP01514J





In this case, the system is no longer isolated since the external power supply is sending electric charges on the electrodes to satisfy (47). Apart from (47), the BCs are complemented by the conditions: $J = 0$, and $K = 0$. The solution of the static equations of the problem are still (7,10,11), where the new integration constants determined by means of the BCs are found to be: $C_0 = 0$, $C_1 = B\cosh[M]$,

$$A = -\frac{V_0}{2\,\sinh[M]}, \quad B = \frac{V_0\Delta\xi - 2(\xi_p + \xi_m)}{2(\xi_m + \xi_p)\cosh[M] + 4\sinh[M]}\,. \tag{48}$$

### A. bulk

Within this framework, $N(z)$, $E(z)$ and $V(z)$ are given by

$$N(z) \;=\; 1 + \frac{[V_0\Delta\xi - 2(\xi_p + \xi_m)]\cosh[z])}{2(\xi_m + \xi_p)\cosh[M] + 4\sinh[M]} - \frac{V_0}{2}\frac{\sinh[z]}{\sinh[M]}, \tag{49}$$

$$E(z) \;=\; \frac{[V_0\Delta\xi - 2(\xi_p + \xi_m)]\sinh[z]}{2(\xi_m + \xi_p)\cosh[M] + 4\sinh[M]} - \frac{V_0}{2}\frac{\cosh[z]}{\sinh[M]}, \tag{50}$$

$$V(z) \;=\; \frac{[V_0\Delta\xi - 2(\xi_p + \xi_m)](\cosh[M] - \cosh[z]) + V_0\,[2 + (\xi_m + \xi_p)\coth[M]]\sinh[z]}{2(\xi_m + \xi_p)\cosh[M] + 4\sinh[M]} \tag{51}$$

In particular in the midplane of the cell ($z = 0$), the electric potential is

$$V(0) = \frac{[V_0\Delta\xi - 2(\xi_p + \xi_m)](\cosh[M] - 1)}{2(\xi_m + \xi_p)\cosh[M] + 4\sinh[M]}$$

which, in the limit of large $M$, i.e., within the HSA, becomes

$$V(0, M \to \infty) = \frac{V_0\Delta\xi - 2(\xi_p + \xi_m)}{2(\xi_m + \xi_p) + 4}\,. \tag{52}$$

In Figure 9, we show the profiles of $N(z)$, $E(z)$ and $V(z)$ for a cell with $\xi_m = 2$, $\xi_p = 5$, $M = 5$ submitted to a potential difference $V_0 = 0.5$.

### B. surface

The surface values of the bulk density of mobile ions are

$$N_{p,m} \;=\; \frac{2\sinh[M] \mp V_0(\xi_{m,p}\cosh[M] + \sinh[M])}{(\xi_m + \xi_p)\cosh[M] + 2\sinh[M]}, \tag{53}$$

View Article Online
DOI: 10.1039/D6CP01514J



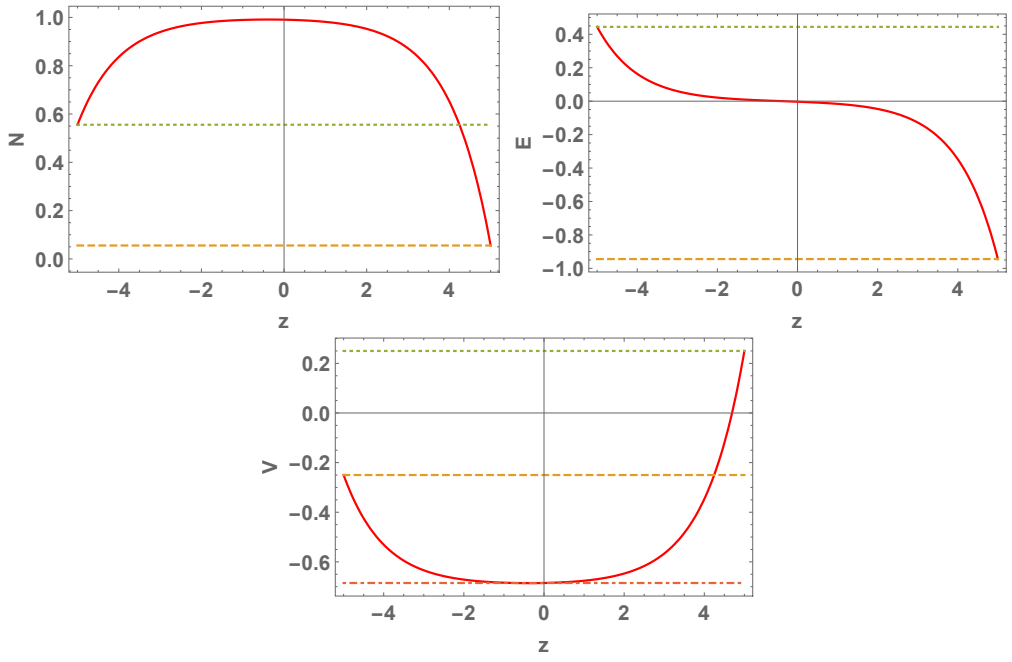


FIG. 9. Bulk ionic density of mobile ions $N$, electric field $E$, and electric potential $V$ vs. $z$ (red curves), due to the ionic adsorption, for a cell with $M = 5$ submitted to an external potential difference $V_0 = 0.5$. Asymmetric cell with $\xi_m = 2$ and $\xi_p = 5$. The horizontal dashed or dotted lines indicate the surface values of the considered quantities. The dashed dotted line marks the value of the electric potential in the midplane of the cell.

that in the HSA become

$$N_{pl,ml} = \frac{2 \mp (\xi_{m,p} + 1)V_0}{2 + \xi_m + \xi_p}. \tag{54}$$

Note that, for an insulating medium, $\Lambda \to \infty$, and hence $M \to 0$. In this limit, the surface values of the bulk densities of the mobile ions tend to

$$N_{p0,m0} = \mp \frac{\xi_{m,p}}{\xi_m + \xi_p} V_0 \,. \tag{55}$$

The dependencies of $N_p$ and $N_m$ on $M$ are shown in Figure 10 where the dashed asymptotes correspond to the HSA.

The equations for the surface electric field are

$$E_{m,p} = -\frac{V_0}{2} \coth[M] \mp \frac{V_0 \Delta\xi - 2(\xi_p + \xi_m)}{2(\xi_m + \xi_p)\cosh[M] + 4\sinh[M]} \sinh[M], \tag{56}$$

which, in the HSA, reduce to

$$E_{ml,pl} = -\frac{V_0}{2} \mp \frac{V_0 \Delta\xi - 2(\xi_p + \xi_m)}{2(\xi_m + \xi_p) + 4}. \tag{57}$$

View Article Online
DOI: 10.1039/D6CP01514J

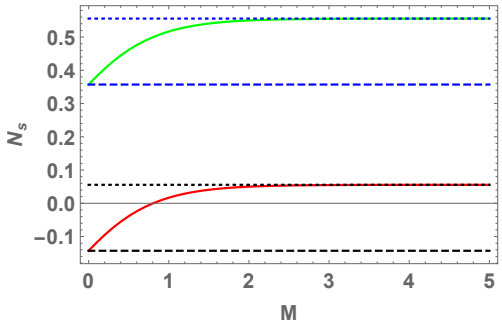


FIG. 10. Surface values of the bulk densities at $z = -M$, in green, and at $z = M$, in red. The curves are drawn for $V_0 = 0.5$, $\xi_m = 2$, and $\xi_p = 5$. The dotted horizontal lines indicate the values given by (55), corresponding to the case $d \ll \Lambda$. The dashed horizontal lines correspond to the HSA, where the surface bulk densities are given by (54).

The dependence of the surface fields $E_m$ and $E_p$ on an applied potential difference and asymmetric adsorption is shown in Figure 11. The horizontal dashed lines are calculated within the HSA.

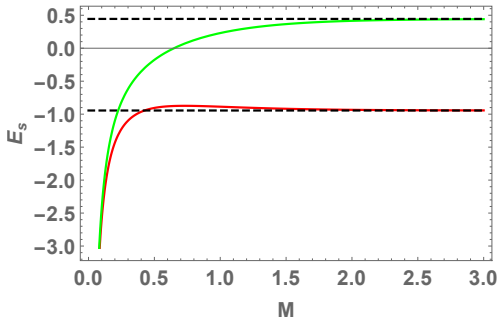


FIG. 11. Surface values of the electric field at $z = -M$, in green, and at $z = M$, in red. The dashed horizontal lines correspond to the HSA, where the surface electric fields are given by (57). The curves are drawn for $V_0 = 0.5$, $\xi_m = 2$, and $\xi_p = 5$.

It is instructive to express the electric field $E$ in absolute units, i.e., to revert to $F$. From the definition of the reduced field $E$, $F$ is given by

$$F = \frac{k_B \Theta}{q \Lambda} E = 2 \frac{k_B \Theta}{q d} M E, \tag{58}$$

where $k_B$ is the Boltzmann constant. Figure 12 shows the same data as Figure 11 with the electric field expressed in absolute units and using the same color code. From (58), in the

View Article Online
DOI: 10.1039/D6CP01514J



limit $M \to 0$, $F$ reduces to

$$\lim_{M\to 0} F = 2\,\frac{k_B\Theta}{qd}\,\frac{V_0}{2} = \frac{v_0}{d}, \tag{59}$$

as expected, since in this limit the medium can be considered as a perfect insulator. The field given by (59) is indicated by the horizontal dashed line in Figure 12. Note that, in the limit as $M \to 0$, the surface fields on the two bounding surfaces are equal and coincide with the bulk value given by (50).

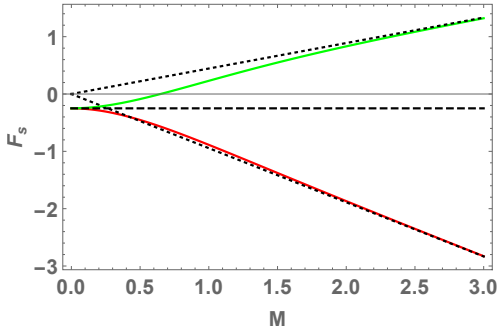


FIG. 12. Surface values of the electric field $F_s = ME_s$, at $z = -M$, in green, and at $z = M$, in red. The dotted lines correspond to the HSA, where the surface electric fields are given by (57). The horizontal dashed line corresponds to the electric field $F_s = v_0/d$, present in an insulating medium. The curves are drawn for $V_0 = .5$, $\xi_m = 2$, and $\xi_p = 5$.

The surface densities of adsorbed ions on the asymmetric electrodes are found by $S_j = \xi_j N_j$, where $N_j$ are given by (53). The electric charge densities sent by the power supply to fix the difference of electric potential between the electrodes at $V_0$ are given by $\Sigma_m = E_m - S_m$ and $\Sigma_p = -(E_p + S_p)$, as it follows from Coulomb's theorem. A simple calculation gives

$$\Sigma_p = \frac{(\xi_m+\xi_p)V_0/\sinh[M] + 2[(\xi_m+\xi_p)V_0 - \Delta\xi + (1+\xi_m\xi_p)V_0\coth[M]]\sinh[M]}{2(\xi_m+\xi_p)\cosh[M] + 4\sinh[M]}, \tag{60}$$

and $\Sigma_m = -\Sigma_p$, as expected.

### C. grounded electrodes

If the electrodes are grounded ($V_0 = 0$), the integration constants become $A = 0$, $C_0 = 0$, $C_1 = B\cosh[M]$, and

$$B = -\frac{\xi_m+\xi_p}{(\xi_m+\xi_p)\cosh[M] + 2\sinh[M]}. \tag{61}$$

View Article Online
DOI: 10.1039/D6CP01514J



In this case, the quantities of interest are:

$$N_{\rm g}(z) \;=\; 1 - \frac{(\xi_m+\xi_p)\cosh[z]}{(\xi_m+\xi_p)\cosh[M]+2\sinh[M]}, \tag{62}$$

$$E_{\rm g}(z) \;=\; -\frac{(\xi_m+\xi_p)\sinh[z]}{(\xi_m+\xi_p)\cosh[M]+2\sinh[M]}, \tag{63}$$

$$V_{\rm g}(z) \;=\; -\frac{(\xi_m+\xi_p)(\cosh[M]-\cosh[z])}{(\xi_m+\xi_p)\cosh[M]+2\sinh[M]} \tag{64}$$

whose surface values are

$$N_{gj} \;=\; \frac{2}{2+(\xi_m+\xi_p)\coth[M]}, \tag{65}$$

$$E_{gm,p} \;=\; \pm\,\frac{\xi_m+\xi_p}{2+(\xi_m+\xi_p)\coth[M]}. \tag{66}$$

The curves $N_{\rm g}(z)$, $E_{\rm g}(z)$ and $V_{\rm g}(z)$ are shown in Figure 8 (black points). $N_{\rm g}(z)$, $E_{\rm g}(z)$ coincide with the corresponding quantities for a short-circuited cell. $V_{\rm g}(z)$ is shifted with respect to $V_{\rm sc}(z)$ by a constant value which corresponds the HSA voltage at the electrodes of a short-circuited cell. All profiles exhibit symmetry even for an asymmetric cell as can be inferred from (62,63,64), for the dependence of the bulk properties on electrodes properties comes only from the sum $\xi_m+\xi_p$. The surface densities, $S_j=\xi_j\,N_j$, of adsorbed particles at the electrodes as a function of $M$, are shown in Figure 13.

We note that $S_p - S_m \sim \Delta\xi$. Therefore, the two curves coincide for a symmetric cell. The surface densities of charges sent by the power supply are

$$\Sigma = \frac{\Delta\xi}{2+(\xi_m+\xi_p)\coth[M]} \tag{67}$$

## VIII. SYMMETRIC SLAB SUBJECTED TO AN EXTERNAL ELECTRIC FIELD

In the symmetric case integration constants $A$ and $C_0$ do not change, whereas $B$ and $C_1$ are found to be

$$B = -\frac{\xi}{\xi\cosh[M]+\sinh[M]}, \quad \text{and} \quad C_1 = -\frac{\xi\coth[M]}{1+\xi\coth[M]} \tag{68}$$

View Article Online
DOI: 10.1039/D6CP01514J

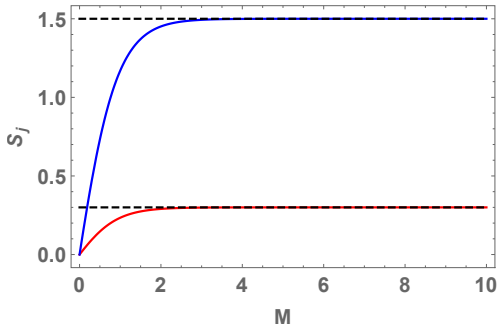


FIG. 13. Surface number densities $S_j$ of adsorbed ions vs. $M$ at the grounded electrodes. $S_m = S(z=-M)$, blue, $S_p$ at $z=M$, red. The dashed horizontal lines correspond to the HSA. $\xi_m = 3$, and $\xi_p = 15$.

In this case the bulk density of mobile ions, the electric field and the electric potential profiles are

$$N(z) = 1 - \frac{\xi\cosh[z]}{\xi\cosh[M]+\sinh[M])} - \frac{V_0}{2}\frac{\sinh[z]}{\sinh[M]}, \tag{69}$$

$$E(z) = -\frac{\xi\sinh[z]}{\xi\cosh[M]+\sinh[M]} - \frac{V_0}{2}\frac{\cosh[z]}{\sinh[M]}, \tag{70}$$

$$V(z) = \frac{2\xi(\cosh[z]-\cosh[M]) + V_0(1+\xi\coth[M])\sinh[z]}{2(\xi\cosh[M]+\sinh[M])}. \tag{71}$$

Figure (14) shows $N(z)$, $E(z)$, and $V(z)$ with $M=5$, for an applied potential difference at the electrodes of $V_0 = 0.5$ (red curves). For comparison, the corresponding functions for cell at open-circuit conditions are plotted in blue. For $V_0 \neq 0$, the symmetry with respect to the midplane of the cell is broken.

The surface values of the bulk densities are given by

$$N_{m,p} = \pm\frac{V_0}{2} + \frac{1}{1+\xi\coth[M]}, \tag{72}$$

whereas the surface values of the electric field by

$$E_{m,p} = -\frac{V_0}{2}\coth[M] \pm \frac{\xi\sinh[M]}{\xi\cosh[M]+\sinh[M]}. \tag{73}$$

Finally, the surface densities of the adsorbed ions are given by $S_j = \xi N_j$.

For the theorem of Coulomb $E_m = \sigma_m = S_m + \Sigma_m$ and $E_p = -\sigma_p = -(S_m + \Sigma_p)$, where $\sigma_m$ and $\sigma_p$ are the total surface density of the adsorbed particles, whereas $\Sigma_m$ and $\Sigma_p$ the surface densities of charges sent by the power supply to fix the electric potential of the

View Article Online
DOI: 10.1039/D6CP01514J



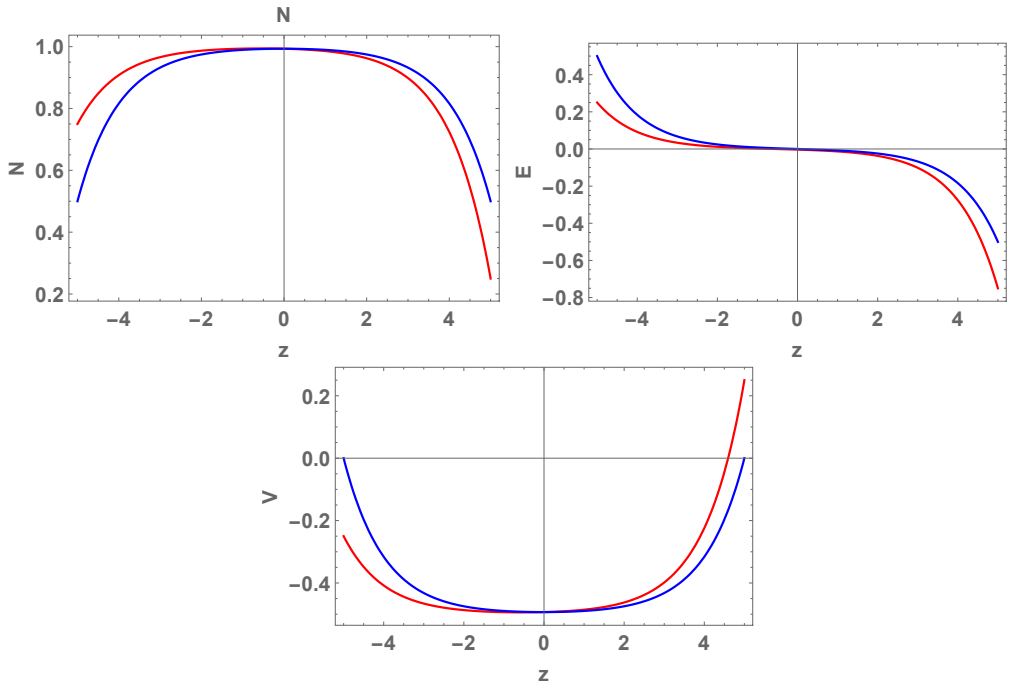


FIG. 14. $N$, $E$, and $V$ vs. $z$ for a symmetric cell with $M = 5$ and $\xi = 1$. In the presence of an external potential difference: $V_0 = 0.5$ (red curves), and in its absence $V_0 = 0$ (blue curves).

electrodes to $V(\pm M) = \pm V_0/2$. It follows that the charges due to the presence of the power supply are

$$\Sigma_m = \Sigma_p = -\frac{V_0}{2}\,(\xi + \coth[M]), \tag{74}$$

proportional to $V_0$. In the particular case where the bounding surfaces are grounded ($V_0 = 0$), the quantities of interest $N_{\rm g}(z)$, $E_{\rm g}(z)$ and $V_{\rm g}(z)$ follow from (69,70,71) respectively, by substituting $V_0 = 0$.

## IX. DISCUSSION AND CONCLUSION

We presented a model that combines PNP equations with the Langmuir kinetic equation to investigate the impact of adsorption in an electrolytic cell at the static regime for both a cell with identical electrodes in what concerns adsorption (symmetric-cell) and a cell with electrodes presenting different adsorption properties (asymmetric-cell). The study was done in the absence and in the presence of an applied dc voltage difference at the electrodes for both open circuit and short circuit cell. The expressions giving the bulk ionic density, electric field and voltage profiles across the thickness of the cell were calculated as well as the surface

View Article Online
DOI: 10.1039/D6CP01514J



values for the density of mobile ions, electric field, voltage, and density of adsorbed ions as functions of the cell thickness over the Debye length ($d/\Lambda$). In the absence of an external bias voltage, an asymmetric cell develops a voltage difference, $\Delta V$, caused by asymmetric adsorption of ions. In this case, it was also shown that the amplitude of $\Delta V$ depends on the reduced thickness $d/\Lambda$ of the cell, and goes to zero for $d << \Lambda$, that is, when exhibiting insulator behavior while on the other limit $d >> \Lambda$, $\Delta V$ tends to a maximum value which is practically attended for $d$ greater than a few $\Lambda$ lengths, that is following the half-space approximation which is valid for $d >> \Lambda$. Similar behavior is shown for the surface values of the mobile ions density, electric field, voltage, and adsorbed ions density. Further, our analysis shows that the voltage difference $\Delta V$ also depends on the adsorption length of the ions, $\ell$, and becomes zero when $\ell$ is the same for both electrodes. In our knowledge, there aren't experimental measurements which could directly be analyzed using the present model. However, deviations of experimental data from the expected behavior which could be attributed to adsorption effects on the electrodes of a cell have been found in impedance spectroscopy measurements where an additional plateau in the limit of the low-frequency range of the real part of the impedance $Z$ was observed [4].

Although our analysis is restricted to static equilibrium of a cell with planar electrodes, the problem remains nontrivial due to the coupling between ionic adsorption, surface charge, and electrostatic fields, which is often neglected or imposed by effective boundary conditions. Extensions of the present analysis using more complex adsorption/desorption mechanisms, distributed kinetics, more than one sign and/or type of mobile ions, or considering frequency dependence, are straightforward but not always analytic solutions exist.

## DECLARATION OF COMPETING INTEREST

The authors declare that they have no known competing financial interests or personal relationships that could have appeared to influence the work reported in this paper.

View Article Online
DOI: 10.1039/D6CP01514J

## DATA AVAILABILITY

Data will be made available on request.





[1] I. Langmuir. The Adsorption of Gases on Plane Surfaces of Glass, Mica and Platinum. J. Am. Chem. Soc., 40 (1918) 1361-1403. doi:10.1021/ja02242a004.

[2] A.W. Adamson, A.P. Gast. *Physical Chemistry of Surfaces*, 6th ed.; Wiley: New York, 1997.

[3] A. Dabrowski. Adsorption from theory to practice. Advances in Colloid and Interface Science, 93 (2001) 135-224.

[4] G. Barbero. Influence of adsorption phenomenon on the impedance spectroscopy of a cell of liquid. Phys. Rev. E71 (2005) 062201.

[5] G. Barbero, L.R. Evangelista, I. Lelidis. Effective adsorption energy and generalization of the Frumkin-Fowler-Guggenheim isotherm. J. Mol. Liq. 327 (2021) 114795. doi:10.1016/j.molliq.2020.114795.

[6] Y. Garbovskiy. A perspective on the Langmuir adsorption model applied to molecular liquid crystals containing ions and nanoparticles. Front. Soft Matter 2 (2022) 1079063. DOI: 10.3389/frsfm.2022.1079063.

[7] R.J. Hunter. *Zeta Potential in Colloid Science*; Academic Press: London, 1981.

[8] R.J. Hunter. *Foundations of Colloid Science*, 2nd ed.; Oxford University Press: Oxford, 2001.

[9] D.F. Evans, H. Wennerström. *The Colloidal Domain: Where Physics, Chemistry, Biology, and Technology Meet*; Wiley-VCH: New York, 1999.

[10] H. Alkhaldia, S. Alharthi, S. Alharthi, H.A. AlGhamdic, et al. Sustainable polymeric adsorbents for adsorption-based water remediation and pathogen deactivation: a review. RSC Adv., 14 (2024) 33143-33190. DOI: 10.1039/D4RA05269B.

[11] G. Zhao, X. Huang, Z. Tang, F. Niu, X. Wang. Polymer-based nanocomposites for heavy metal ions removal from aqueous solution: a review. Polym. Chem. 9 (2018) 3562-3582. doi:10.1039/C8PY00484F.

[12] Lazar MM, Ghiorghita CA, Dragan ES, Humelnicu D, Dinu MV. Ion-Imprinted Polymeric Materials for Selective Adsorption of Heavy Metal Ions from Aqueous Solution. Molecules. 2023 Mar 20;28(6):2798. doi: 10.3390/molecules28062798.

View Article Online
DOI: 10.1039/D6CP01514J



[13] C.M. Schott, P.M. Schneider, K.-T. Song, H. Yu, R. Götz, et al. How to Assess and Predict Electrical Double Layer Properties. Implications for Electrocatalysis. Chem. Rev. 124 (2024) 12391-12462. doi: 10.1021/acs.chemrev.3c00806.

[14] B.E. Conway. *Electrochemical Supercapacitors*; Kluwer Academic/Plenum: New York, 1999.

[15] W. Schmickler, E. Santos. *Interfacial Electrochemistry*; Springer: Berlin, 2010.

[16] K. Nakanishi, T. Sakiyama, K.J. Imamura. On the Adsorption of Proteins on Solid Surfaces. Biosci. Bioeng. 91 (2001) 233–244. doi: 10.1016/S1389-1723(01)80127-4.

[17] M. Rabe, D. Verdes, S. Seeger. Understanding Protein Adsorption Phenomena at Solid Surfaces. Adv. Colloid Interface Sci. 162 (2011) 87–106. DOI: 10.1016/j.cis.2010.12.007.

[18] W. Norde. In *Proteins at Liquid Interfaces*; ACS Symp. Ser. 1120 (2012) 1–14. DOI: 10.1021/bk-2012-1120.ch001.

[19] K.Y. Foo, B.H. Hameed. Insights into the Modeling of Adsorption Isotherm Systems. Chem. Eng. J. 156 (2010) 2–10. DOI: 10.1016/j.cej.2009.09.013.

[20] G. Crini, E. Lichtfouse. Advantages and Disadvantages of Techniques Used for Wastewater Treatment. Environ. Chem. Lett. 17 (2019) 145–155. DOI: 10.1007/s10311-018-0785-9.

[21] P. Simon, Y. Gogotsi. Materials for Electrochemical Capacitors. Nat. Mater. 7 (2008) 845–854. DOI: 10.1038/nmat2297.

[22] K. Xu. Electrolytes and Interphases in Li-Ion Batteries and Beyond. Chem. Rev. 114 (2014) 11503–11618. DOI: 10.1021/cr500003w.

[23] Y. Bai, N.L. Abbott. Recent Advances in Colloidal and Interfacial Phenomena Involving Liquid Crystals. Langmuir 27 (2011) 5719-5738. dx.doi.org/10.1021/la103301d.

[24] E. Iakovleva, M. Sillanpää in *Novel sorbents from low-cost materials for water treatment. Advanced Water Treatment*, ch.4, 2020 265-359.

[25] S. Bousiadi, I. Lelidis. Asymmetric adsorption in an open electrolytic cell. Phys. Lett. A 382 (2018) 127-134. doi: 10.1016/j.physleta.2017.10.050.

[26] S. Chen, H. Dong, J. Yang. Surface Potential/Charge Sensing Techniques and Applications. Sensors 20 (2020) 1690. doi:10.3390/s20061690.

[27] J.O'M. Bockris, A.K.N. Reddy, *Electrodics in Chemistry, Engineering, Biology and Environmental Science*, Modern Electrochemistry 2B (Kluwer Academic Publishers, 2004).

[28] M.E. Orazem, B. Tribollet, *Electrochemical Impedance Spectroscopy* (Wiley, 2008).

View Article Online
DOI: 10.1039/D6CP01514J



[29] G. Barbero, L.R. Evangelista, *Adsorption Phenomena and Anchoring Energy in Nematic Liquid Crystals*, (CRC Press, 2005).

[30] A.Ch. Lazanas, M.I. Prodromidis. Electrochemical Impedance Spectroscopy- A Tutorial. ACS Meas. Sci. Au 3 (2023) 162-193. doi: 10.1021/acsmeasuresciau.2c00070.

[31] G. Barbero, A.L. Alexe-Ionescu. Role of the diffuse layer of the ionic charge on the impedance spectroscopy of a cell of liquid. Liq. Cryst. 32 (2005) 943-949. doi:/10.1080/02678290500228105.

[32] I. Lelidis, J.R. Macdonald, G. Barbero. Poisson-Nernst-Planck model with Chang-Jaffe, diffusion, and ohmic boundary conditions. J. Phys. D: Appl. Phys. 49 (2016) 025503-1-11.

[33] M. Samet, V. Levchenko, G. Boiteux, G. Seytre, A. Kallel, A. Serghei, J. Chem. Phys. 142 (2015) 194703-1-12

[34] H. Dechiraju, M. Jia, L. Luo, M. Rolandi. Ion-Conducting Hydrogels and Their Applications in Bioelectronics. Adv. Sustainable Syst. 6 (2022) 2100173. DOI: 10.1002/adsu.202100173.

[35] X. Zhang, Y. Tang, P. Wang, Y. Wang, T. Wu, et al. A review of recent advances in metal ion hydrogels: mechanism, properties and their biological applications. New J. Chem. 46 (2022) 13838-13855. DOI: 10.1039/d2nj02843c.

[36] P.W. Atkins, *Physical Chemistry*, Oxford University Press, Oxford, 2000.

[37] J.N. Israelachvili, *Intermolecular and Surface Forces*, 3rd ed., Academic Press, London, 2011.

[38] I Lelidis, G Barbero. A generalization of the linear adsorption model to include electrosorption. Colloids and Surfaces A: Physicochemical and Engineering Aspects 678 (2023) 132440. doi:10.1016/j.colsurfa.2023.132440.

[39] I. Lelidis, G. Barbero, A. Sfarna. Comparison of two generation-recombination terms in the Poisson-Nernst-Planck model. J. Chem. Phys. 137 (2012) 154104-1-10.

[40] L. D. Landau et E. I. Lifchitz, *Electroynamique des milieux continus*, MIR, Moscow, 1960.

[41] G. Barbero, I.Lelidis. Evidence of the ambipolar diffusion in the impedance spectroscopy of an electrolytic cell. Phys. Rev. E 76 (2007) 051501-1-9.

[42] B. Riechers, F. Maes, E. Akoury, J.-C. Baret. Surfactant adsorption kinetics in microfluidics. Edited by David A. Weitz, Harvard University, Cambridge, MA, 113 (2016) 11465-11470. doi.org/10.1073/pnas.1604307113.

[43] O. Pecina and J.P. Badiali. Electrostatics of a modulated membrane with specific adsorption. Phys. Rev. E 60 (1999) 4431.

View Article Online
DOI: 10.1039/D6CP01514J



[44] P. Massé, E. Sellier, V. Schmitt, V. Ravaine. Impact of Electrostatics on the Adsorption of Microgels at the Interface of Pickering Emulsion. Langmuir 30 (2014) 14745-14756. doi: 10.1021/la503040f.

[45] M. Tepermeister, N. Bosnjak, J. Dai, X. Zhang, S.M. Kielar, et al. Soft Ionics: Governing Physics and State of Technologies. Front. Phys. 10 (2022) 890845. doi: 10.3389/fphy.2022.890845.

[46] H. Dechiraju, M. Jia, L. Luo, M. Rolandi. Ion-Conducting Hydrogels and Their Applications in Bioelectronics. Adv. Sustainable Syst. 6 (2022) 2100173.Doi: 10.1002/adsu.202100173.

[47] Li, H.; Eddaoudi, M.; O'Keeffe, M.; Yaghi, O. M. Design and Synthesis of an Exceptionally Stable and Highly Porous Metal-Organic Framework. Nature 402 (1999) 276–279. DOI: 10.1038/46248.

[48] Furukawa, H.; Cordova, K. E.; O'Keeffe, M.; Yaghi, O. M. The Chemistry and Applications of Metal-Organic Frameworks. Science 341 (2013) 1230444. DOI: 10.1126/science.1230444.

[49] G. Barbero; I. Lelidis. Effective dielectric constant of electrolytes. J. Appl. Phys. 115 (2014) 194101 . doi.org/10.1063/1.4875837.

[50] S. Tripathi, S.N. Tan, A. Bhattacharya, R.F. Tabor. Measuring and modelling the adsorption kinetics of polydisperse PiBSA-based emulsifiers using dynamic interfacial tension measurements. Colloids Surf. A Physicochem Eng. Asp. 624 (2021) 126728. doi.org/10.1016/j.colsurfa.2021.126728.

[51] D. Cignolo, V. Rizzi, P. Fini, A. Petrella, C. Milanese, P. Cosma, J. Gubitosa, Composite Chitosan-Biochar-based sponges for the removal of Direct Blue-78 from water: Physical and chemical parameters affecting the adsorption process. Colloids Surf. A Physicochem Eng. Asp. 724 (2025) 137518. doi.org/10.1016/j.colsurfa.2025.137518.

[52] B. Maximus, E. De Ley, A. De Meyere, H. Pauwels. Ion transport in SSFLCD's. Ferroelectrics, 121 (1991) 103-112. https://doi.org/10.1080/00150199108217614

[53] B. Maximus, C. Colpaert, A. de Meyere, H. Pauwels. Transient leakage current in nematic LCDs. Liq. Cryst. 15 (1993) 871-882. doi.org/10.1080/02678299308036506

[54] Y. Huang, P.J. Bos, A. Bhowmik. The ion capturing effect of 5Â° SiOx alignment films in liquid crystal devices. J. Appl. Phys. 108 (2010) 064502.

View Article Online
DOI: 10.1039/D6CP01514J

**Data availability**

Data will be made available on request.